JOURNAL OF GEOPHYSICAL RESEARCH, VOL. 104, NO. E5, PAGES 11,853–11,864, MAY 25, 1999

The gravitational and aerodynamic sorting of meteoritic chondrules and metal: Experimental results with implications for chondritic meteorites

D. Glen Akridge and Derek W. G. Sears

Cosmochemistry Group, Department of Chemistry and Biochemistry, University of Arkansas, Fayetteville

Abstract. Chondritic meteorites appear to have undergone metal-silicate fractionations and chondrule size sorting that resulted in unique distributions for each chondrite class. We present evidence from laboratory experiments for size sorting of meteoritic chondrules and metal by fluidization during parent body degassing caused by evaporation and sublimation of water in the parent bodies. Experiments using chondritic analogs in an upward flowing stream of air indicate that metal can travel upward in a fluidized bed, resulting in a metal-rich surface and metal-poor regions at depth. When the outgassing velocity drops below the minimum fluidization velocity for chondrules, metal grains still suspended in the gas travel upward through the pore spaces between chondrules, provided the size ratio between chondrules and metal is >3. These experiments also suggest that chondrule size sorting can occur but with less efficiency than metal-silicate sorting. Fluidization can account for the sorting observed in enstatite chondrites, suggesting that only one parent body is required for EH and EL chondrites. Ordinary chondrite components are also sorted, with H chondrites deriving from locations near the surface of the parent body, while L and LL chondrites originate from greater regolith depths. The upward migration of metal to asteroid surfaces may help explain the reddened spectral features of asteroids likely to be the parent bodies of ordinary chondrites.

1. Introduction

Particle sorting can arise by shaking, vibrating, pouring, or fluidizing a mixture of granular materials. The degree of segregation depends on material properties of the granules such as size, density, shape, and particle resilience [*Williams,* 1976]. The greater the material differences among particles the more efficient the segregation. For fluidized systems in which a gas is passed upward through a bed of particles, the separation of granules depends upon the relative gas drag experienced by each particle. When the gas reaches a minimum fluidization velocity, the bed attains fluid-like characteristics and the particulate solids are free to move according to their physical properties. In general, larger and heavier particles tend to settle out of a gas stream before smaller and lighter particles. This type of segregation is an important aspect of many processes in engineering and geophysics. Industrial applications of fluidized beds commonly involve solid particulate material acting as a substrate for gas-solid reactions [*Kunii and Levenspiel,* 1991]. The realization of graded bed deposition following pyroclastic flows has led many to suspect that size sorting can occur within the expanding gas cloud [*Wilson,* 1980, 1984; *Carey,* 1991]. The flow of a gas-solid cloud away from a volcanic vent will continue as long as the gas velocity is large enough to overcome gravitational forces. *Hoblitt et al.* [1981] found that median grain size decreased with increasing pyroclastic flow distance in the ignimbrite deposits from the 1980 Mount St. Helens eruption. *Newsom et al.* [1986] reported degassing pipes in the suevite deposits surrounding the Ries impact crater in Germany. The cylindrical pipes were devoid of fine-grained material and were assumed to have been elutriated by the initially fluidized suevite.

Huang et al. [1996a] have previously suggested that the metal-silicate fractionations observed in chondritic meteorites may have arisen by fluidization mechanisms during parent body degassing. The Huang et al. proposal is that impact or radiogenic heating of water-rich asteroids can drive off large amounts of volatiles, creating a dynamic surface dust layer in which chondrules and metal grains can be sorted according to size and density. Each chondrite class has a unique size range for chondrules and metal (Table 1), suggesting different formational processes or subsequent sorting. Iron abundance and oxidation state also varies among meteorite classes (Figure 1). We suspect that parent body degassing of water and other volatiles along with chondrule and metal grain sorting could be one of the major factors in determining many of the properties observed in chondritic meteorites. In this paper we explore the feasibility of fluidized size-sorting of chondritic components as originally outlined by *Huang et al.* [1996a] using laboratory experiments as an analog for meteorite parent body surfaces. Experiments are needed to quantify the efficiency of gravitational and aerodynamic sorting, since many previously proposed sorting mechanisms involve nebula separation of chondrules and metal and have failed to completely explain the observed size and abundance patterns in meteorites.

2. Previous Models for Metal-Silicate Fractionation

Urey [1961] argued that metal-silicate fractionations could not occur on parent bodies since this required melting, and

Copyright 1999 by the American Geophysical Union.

Paper number 1999JE900021.
0148-0227/99/1999JE900021$09.00

Table 1. Mean Physical Properties of the Major Chondrite Classes

	H	L	LL	EH	EL	CO	CV	CM	CI	Ref.
Chondrule diameter, mm	0.3	0.7	0.9	0.25	0.5	0.25	1.0	0.3	-	1,2
Metal diameter, mm*	0.19	0.16	0.14	0.04	0.1	-	-	-	-	2,3
Chondrule abundance, vol%	65-75	65-75	65-75	20-40	20-40	35-40	35-45	<15	0	1
Metal abundance, wt%	16	7	2.4	22	18	2.3	0.16	0.14	0	4
Matrix abundance, vol%	10-15	10-15	10-15	<5	<5	30-40	40-50	~60	100	1
water, wt%	0.44	0.46	0.71	1.59	0.59	3.27	0.25	10.4	16.9	4

References are 1, *Grossman et al.* [1988]; 2, *Schneider et al.* [1998]; 3, *Dodd* [1976]; 4, *Jarosewich* [1990].

*Metal diameters for H, L, and LL were taken from *Dodd* [1976] and include data for nonisolated metal grains. The mean isolated metal grain size for H, L, and LL is probably less than that shown in the table. *Benoit et al.* [1998] found the mean isolated metal grain size for Sharps (H3.4) to be 0.065 mm.

chondritic textures are clearly not the result of melting. Since that time, metal-silicate fractionation models have largely focused on nebular processes [*Newsom*, 1995] to explain the Fe/Si trends found in chondrites. Earlier models suggested metal-silicate sorting could occur by different accretion efficiencies onto parent bodies [*Donn and Sears*, 1963; *Orowan*, 1969] or through magnetic interactions in the nebula [*Larimer and Anders*, 1970]. *Larimer and Wasson* [1988] suggested that fractionations could occur through the differential settling of components to the nebular midplane. Certainly the most popular method of fractionating meteoritic components has grown out of aerodynamic sorting originally postulated and quantified by *Whipple* [1971, 1972]. *Weidenschilling* [1977] generalized Whipple's results to include all solid objects moving through a gas. *Dodd* [1976] used Whipple's equations for gas drag to determine if the components of ordinary chondrites had been acrodynamicallly sorted. Despite obtaining results that disagreed with the gas drag equations, Dodd concluded that aerodynamic sorting was still the most viable method for sorting meteoritic components. *Clayton* [1980] argued that fractionation of refractory elements could occur according to grain size during condensation in the nebula. *Liffman and Brown* [1995, 1996] used the particulate size data published for ordinary and CR chondrites to conclude that protostellar "jets" of material can create similar aerodynamic sorting efficiencies for the chondrite classes. Qualitative arguments for aerodynamic sorting of chondrules and metal in L chondrites [*Rubin and Keil*, 1984], CR chondrites [*Skinner and Leenhouts*, 1993], and the ordinary chondrites as a whole [*Haack and Scott*, 1993; *Scott and Haack*, 1993] have been proposed. *Cameron* [1995] postulated aerodynamic sorting by radial drift through the nebula but incorrectly compares the resultant sorting to that of the fluidized bed model described by *Sears et al.* [1994] for planetesimal surfaces.

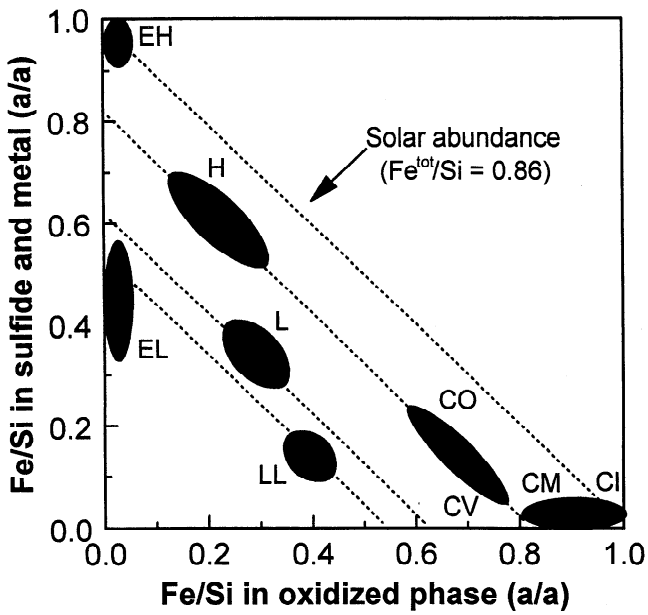

Figure 1. Urey-Craig plot showing Fe oxidation states for the major chondrite classes. Dashed lines represent possible redox trends. The ordinary chondrites differ in redox characteristics and the abundance of Fe. H chondrites are more reduced and have greater Fe content than L or LL. Enstatite chondrites are extremely reduced but are fractionated in their total iron content. Fields drawn from data of *Wasson* [1985].

3. Problems With Nebula Sorting Models

Size sorting of particulates by movement through the nebula gas is an appealing and simple model for metal-silicate fractionation, but one requiring major assumptions about nebula conditions. One essential requirement for these models is the presence of chondrules early in the disk evolution process. However, it now appears that chondrules in ordinary chondrites were forming up to 6 Ma after after the first formed solids (calcium-aluminum inclusions) [*Hutcheon et al.*, 1994; *Swindle et al.*, 1996]. Chondrule formation appears to span the total lifetime of the solar nebula [*Podosek and Cassen*, 1994] and limits the potential for aerodynamic sorting of chondrules in the nebular gas. Since nebula gas pressures were low (~10^{-5} atm), aerodynamic sorting would require nebula-wide movement of solids [e.g., *Cameron*, 1995; *Shu et al.*, 1996]. *Liffman and Brown* [1996], for example, argue for chondrule formation within 0.1 AU of the protosun followed by ejection in a jet of solar wind. It is difficult to conceive how widespread movement of solids in the nebula could form and preserve meteorite classes with distinct oxygen isotope abundances [*Clayton et al.*, 1976] and petrographic properties [*Wood*, 1985].

Aerodynamic sorting can occur by one of two regimes [*Whipple*, 1972]. The Stokes drag regime is applicable for a dense gas in which the mean free path of gas molecules is short relative to the diameter of the particle. When the mean free path is large relative to particle diameter the Epstein drag law is in effect. By equating the Stokes and Epstein drag regimes, *Dodd* [1976] was able to develop a simple relationship for testing aerodynamic sorting:

$$\rho_m d_m^x = \rho_{si} d_{si}^x \quad (1)$$

where x equals 1 for Epstein drag and 2 for Stokes drag and ρ_{si} and d_{si} are the density and diameter of the average silicate particle and ρ_m and d_m are the density and diameter of the average metal grain in a given meteorite. For aerodynamic sorting the calculated value of x for any chondrite should fall

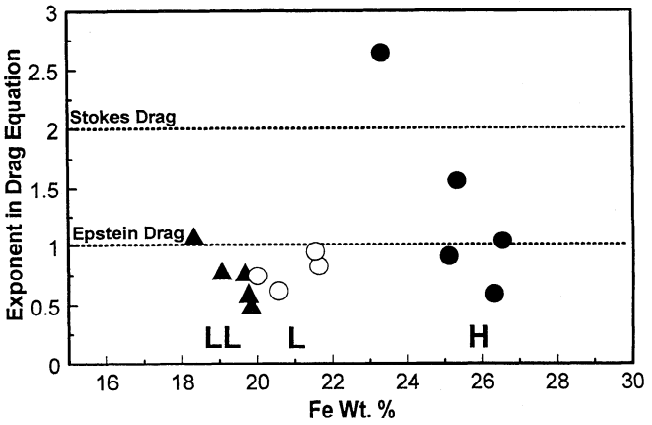

Figure 2. Plot of the exponent in the expression $\rho_m d_m^x = \rho_s d_s^x$ for coexisting metal and chondrules in ordinary chondrites. When the mean free path of the gas molecules is greater than the particle diameters, Epstein's law applies and $x = 1$, but when the mean free path is short relative to the particle diameter, Stokes' law applies and $x = 2$. The data for chondrules and metal do not cluster around values of 1 or 2; they spread both above and below these values. This suggests that acrodynamic drag alone cannot explain the size sorting of coexisting grains in ordinary chondrites. (Chondrule data from *Benoit et al.* [1998], *Hughes* [1978], *Huang et al.* [1996b], and *King and King* [1979]. Metal data from *Benoit et al.* [1998] and *Dodd* [1976].)

within the limits for the two drag regimes, with values near 1 expected for the low density nebula. *Dodd* [1976] applied this relationship to metal and silicate grains in ordinary chondrites and found x values ranging from 0.75 to 4.6. The scattering of data below 1 and well above 2 clearly implies that the components of ordinary chondrites were not sorted by aerodynamic processes alone [*Sears and Akridge*, 1998]. If the same relationship is used for chondrules and metal only, a similar result is obtained (Figure 2). The values for L and LL chondrites fall below that expected for Epstein drag, whereas H chondrites plot below, between, and above the values predicted from the aerodynamic equations. Aerodynamic sorting also does not adequately explain the metal abundance found in chondrites (Table 1). For example, EL chondrites are depleted in metal relative to EH and solar values (Figure 1). If small particles are being aerodynamically size-sorted in the nebula, an additional process must be invoked to account for the distribution of metal.

Several authors have mistakenly assumed that *Dodd's* [1976] tabulation of silicate grain sizes in ordinary chondrites represented chondrules [e.g., *Martin and Mills*, 1976; *Liffman and Brown*, 1996]. However, as pointed out by *Martin and Mills* [1978], Dodd actually measured all silicates including droplet, irregular, and fragmented chondrules and matrix grains. *Liffman and Brown* [1996] misused *Dodd's* [1976] silicate data to support their model of mass equivalence during aerodynamic sorting:

$$\frac{\rho_m}{\rho_{si}} = \frac{d_{si}}{d_m} Q(r) \qquad (2)$$

where $Q(r)$ is a velocity dependent term assumed to be equal to 1. Since the density of metal grains is approximately twice that of silicates (they used ρ_m = 7.8 g cm^{-3} and ρ_{si} = 3.8 g cm^{-3}), it was reasoned that the metal/chondrule size ratio should be $\approx$ 0.5. When using Dodd's data for ordinary chondrites and data for CR chondrites [*Skinner and Leenhouts*, 1993], they found the metal/"chondrule" ratio to be 0.52±0.16. However, when using actual chondrule size data from Table 1, the ratios should be H=0.63, L=0.23, LL=0.16, EH=0.16, EL=0.20.

We believe the problems outlined above for nebula sorting of chondrule and metal grains warrant investigation of alternative processes. Fluidization on parent body surfaces differs from aerodynamic sorting by requiring an upward stream of gas to "lift" a particle against gravitational forces. The high particle densities in a fluidized bed result in repeated collisions among grains and prevent particle behavior based on simple aerodynamic drag. Bed dynamics and sorting are governed by the characteristics of the entire bed and are not dependent on the properties on any given particle.

4. Experimental Procedure

Experiments were carried out in a Plexiglas tube 2.5 cm in diameter and 80 cm in length (Figure 3). An airflow at room temperature was passed upward through the tube containing various mixtures of particulate material (primarily quartz and iron). In-line flow meters were used to measure air velocities between 0 and 195 cm/s (0-970 mL/s). A diffuser was constructed in order to distribute the air evenly upon entrance into the tube. The diffuser consisted of a Plexiglas plate containing holes of 2 mm diameter underlying a 10 mm thick bed of cotton. Pressure drop across the bed was measured using a water manometer constructed of glass tubing. Ten access holes each with a diameter of 6 mm were placed vertically along the column at approximately 15 mm intervals. The holes allowed removal of material for analysis after each fluidization run. Typical fluidization runs involved placing one or more weighed components into the column. Each component had

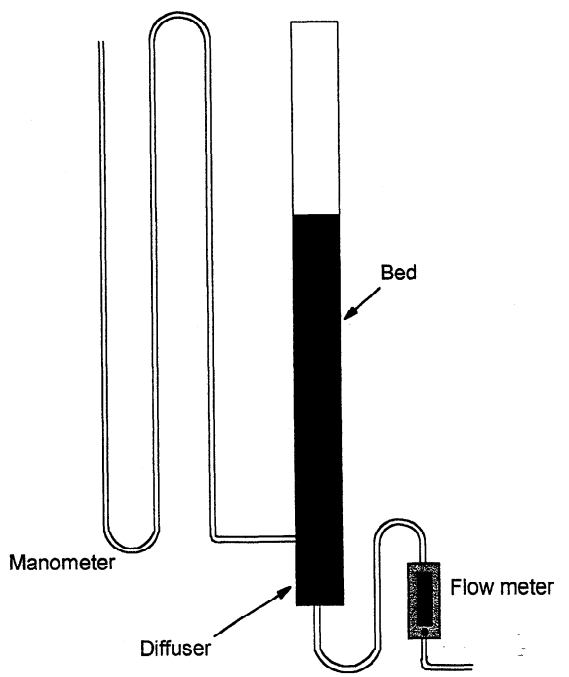

Figure 3. Schematic of fluidized bed. Airflow measured by in-line flow meters enters the column through a diffuser. Pressure drop across the bed is measured using a water manometer.

Table 2. Properties of Meteoritic Components and Laboratory Analogs

	Size Range, μm	Density, g cm^{-3}	Aspect Ratio*
Meteoritic component			
Chondrules	200-1000	3.2	1.2 - 1.4†
Metal	40-200	8	1.3 - 2.2†
Laboratory Analog			
Quartz sand	200-1000	2.6	1.4 ± 0.3
Iron	50-200	7.9	1.4 ± 0.4

*Ratio of largest to smallest diameters; errors are 1σ. See text for measurement details.
†Meteoritic aspect ratios based on in-house data collected from H3 (Sharps); EL3 (ALH 85119, MAC 88180, PCA 91020); and EH3 (ALH 84170, PCA 91085, PCA 91238) meteorites.

been previously screened through a variety sieves to obtain particulates of the desired size range. Volume fractions within the column were recorded by noting the bed height of each component. High gas flow rates were used to obtain a uniformly mixed bed. Gas flow rates of specific and varying velocities allowed for the segregation of bed components. In some cases a video camera was used to record the physical movement of particles within the bed. After a fluidization run, ~1 g samples were removed from each access hole for analysis going from the top down to avoid disturbing the bed components. Each sample removed could be separated into weighed fractions by magnetic removal of iron grains from the silicate grains. An average particle mass was determined by weighing 100 grains from each fraction. An average particle volume and radius was determined by conversion of the average particle mass using grain density and assuming sphericity. The effects of wall drag on the gas flow were not considered since previous engineering studies determined that bed dynamics were unaffected when the bed diameter is ≥ 10 times the largest particle diameter [*Kunii and Levenspiel*, 1991]. The largest particles studied were ~1 mm, which gives a bed/particle ratio of 25.

The components used as analogs for chondritic components were quartz sand and iron powder (Table 2). Particle densities were similar, and the analog sizes prior to fluidization were controlled by sieving. Comparing the overall shape characteristics is more difficult, since the sizes of chondritic components are usually measured in a two-dimensional thin section, whereas the chondritic analogs are three-dimensional particles. We suggest the closest possible comparison that can be made regarding shape characteristics is through aspect ratios. Our lab has previously measured the aspect ratios of chondrules and isolated metal grains in unmetamorphosed ordinary (Sharps) and enstatite (ALH 84170, PCA 91085, PCA 91238, ALH 85119, MAC 88180, PCA 91020) chondrites. Aspect ratios were determined by taking the mean of the grain's long and semimajor axis using a calibrated microscope reticule under transmitted light. A similar procedure was used (albeit less precise) for measuring the long and short axis of the three-dimensional chondritic analogs. Table 2 compares the aspect ratios for grains in Sharps (H3.4) and those for quartz and iron. Chondrules appear to be slightly more rounded on average than quartz grains, but there is good agreement between metal and iron grains. However, aspect ratios for meteoritic metal grains can range as high as 2.2 ± 1.1 in EL3 chondrites (ALH 85119). Although particle shape does play a role in determining fluidization behavior, we stress that the minor shape differences between meteoritic and analog grains will not greatly effect results, since high collision rates between grains in a fluidized bed limit aerodynamic drag effects based on shape characteristics.

5. Results for Chondritic Analogs

The minimum flow rate required for initial fluidization of chondritic-like particles (Table 2) was determined empirically by measuring the pressure drop across the bed. As the gas flow through the solids is increased, the pressure differential between the bottom and surface of the bed grows linearly with flow rate (Figure 4). At the minimum fluidization velocity v_{mf} the bed

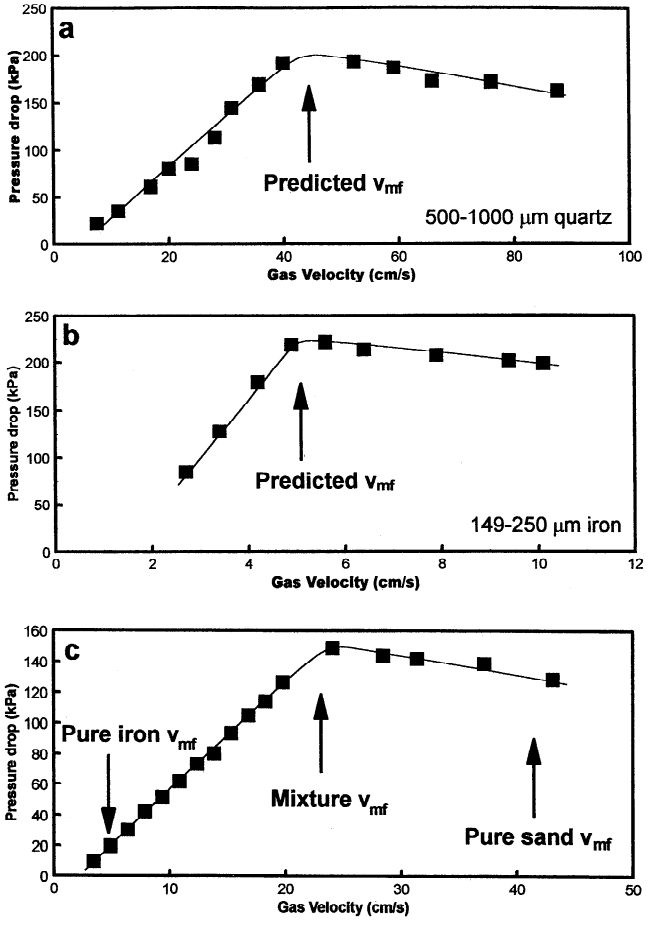

Figure 4. Fluidization plots for chondritic analogs. Pressure drop, measured as a function of bed height, increases proportionally to the gas velocity until the minimum fluidization velocity is reached. Predicted v_{mf} was calculated using (A1). (a) Minimum flow rate for quartz sand (500-1000 μm) is 43 cm/s. (b) Iron (149-250 μm) has v_{mf} = 5 cm/s. (c) The onset of minimum fluidization for a mixture of sand and iron is intermediate between the v_{mf} for the two bed components.

expands and deforms, minimizing pressure differences throughout the bed [*Kunii and Levenspiel*, 1991]. The onset of a bubbling bed results in the leveling off or a slight decrease in the pressure differential. Figures 4a and 4b are experimental fluidization runs showing the minimum fluidization velocities of 500-1000 μm sand and 149-250 μm iron grains. Both runs agree well with the v_{mf} predicted by (A1). The gas velocity for minimum fluidization is about a factor of 10 greater for the larger quartz sand than for iron. The minimum fluidization velocity is primarily dependent on particle size [*Chiba et al.*, 1980]:

$$v_{mf} \propto d^2 \rho_s \quad (3)$$

in the near laminar flow region. The v_{mf} of a mixture of quartz and iron grains (Figure 4c) lies between that of the pure components. In this case, the mixture v_{mf} is nearly the mean of the pure components, but the mixture v_{mf} can be any intermediate value depending upon grain sizes and their fractional abundance.

The segregation of particulate material is a function of size and density. Conventional wisdom for industrial applications suggests that in binary mixtures the denser component will become jetsam and the lighter component will become flotsam [*Rowe and Neinow*, 1976; *Delebarre et al.*, 1994]. The experiments by *Rowe et al.* [1972a,b] indicated that even order of magnitude differences in particle sizes showed only slight segregation tendencies. One reason for this is that when large particles are in a bed of smaller particles the larger will behave as flotsam if its intrinsic density is less than the bulk density of the smaller bed particles [*Nienow et al.*, 1978]. Thus some large particles tend to sink while others rise. In chondritic meteorites the size and density of two of the primary components (chondrules and metal) are unique in that they have large size and density differences and that the denser component (metal) comprises <20% by weight. The fluidization characteristics of chondritic material can not be determined by extension of industrial applications.

We examined the fluidization behavior of numerous chondritic-like mixtures to determine their segregation behavior. The segregation of metal in a single run can be determined by plotting the weight percent of metal as a function of bed height.

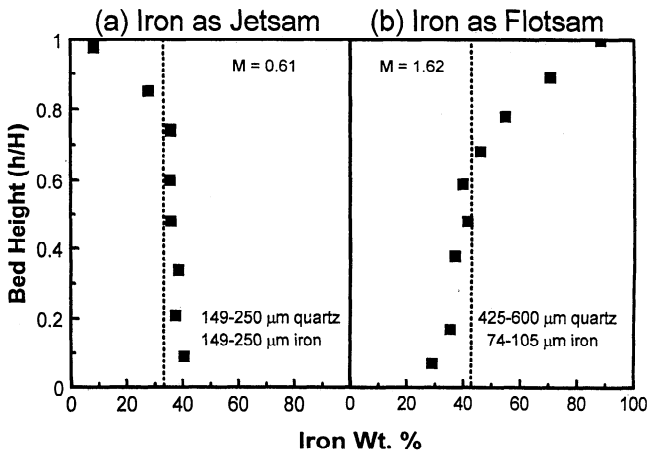

Figure 5. Segregation plots for iron. (a) Iron behaves as jetsam whenever similar sized quartz/sand mixtures are fluidized. (b) Iron behaves as flotsam whenever the iron size is considerably smaller than quartz. The mixing index M is also given for each segregation plot (see text for details).

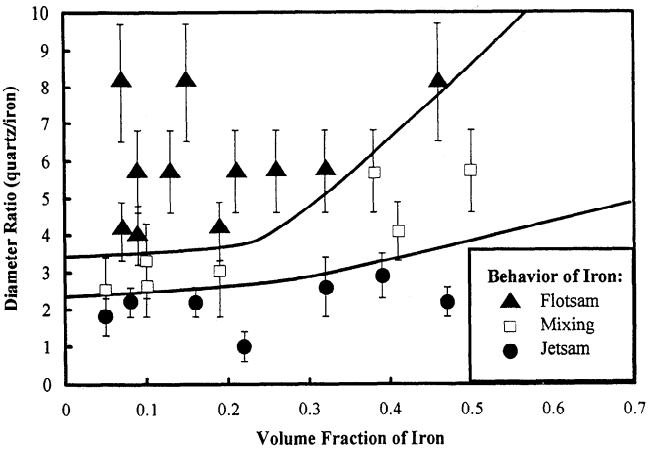

Figure 6. Segregation plot showing the behavior characteristics of iron during slow degassing for a variety of quartz/iron mixtures. When iron volume fractions are < 20%, the iron becomes flotsam whenever the particle size ratio is > 3. Size ratios < 2 generally result in the iron behaving as jetsam during fluidization.

The degree of metal segregation can be determined by the mixing index

$$M = x/x_H \quad (4)$$

where x is the metal fraction in the upper part of the bed and x_H is the average metal fraction in the entire bed [*Kunii and Levenspiel*, 1991]. If metal is jetsam, then $0 \le M \le 1$. If the metal is flotsam, then $1 \le M \le 1/x_H$. Perfect mixing corresponds to M = 1, and complete segregation occurs at M = 0 and M = $1/x_H$.

Experiments involving quartz sand and iron grains show that particle size is extremely important in determining the bed behavior. When particles of similar sizes are fluidized, the denser iron became jetsam and was enriched in the lower regions of the bed. Figure 5a shows the final bed segregation of similar sized quartz and iron grains. The mixing index for this fluidization run was 0.61, indicating significant depletion of iron in the upper 20% of the bed. In contrast, when the quartz to iron size ratio was increased, the opposite trend in segregation began to occur. During the terminal stages of degassing, iron grains migrated upward to form iron-rich surface regions. Figure 5b indicates that for a quartz/sand size ratio of 5.7, the bed surface regions can contain up to 90 wt% iron after fluidization. The mixing index for Figure 5b is 1.62, a strongly segregating system. The efficiency of particle segregation depends largely on gas velocity. Exceedingly high velocities ($>3v_{mf}$) serve to mix the bed components. Gas velocities at or near the v_{mf} can effectively segregate binary mixtures if their size and density differences are sufficiently different. Maximum segregation as observed in Figures 5a and 5b occurs by slowly reducing the gas velocity from >3 v_{mf} to 0 v_{mf}. As the gas flow is reduced below the v_{mf} for quartz, the quartz grains settle out of the gas stream and become stationary objects. If the quartz/iron size ratio is large, the iron grains can travel upward through the pore spaces of the quartz, resulting in an iron-rich surface. When the size ratio is similar, the more familiar pattern of the denser particle sinking in the bed occurs.

To understand the sorting tendencies of quartz and iron grains, a segregation map (Figure 6) was prepared that indicates the behavior of iron grains for binary systems containing various size ratios and iron abundances. Iron behaves as flotsam if the

Table 3. Experimental Results for the Separation of Metal and Quartz in a Fluidized Bed

Run	Volume Fraction of Metal	Metal Grain Size, μm	Quartz Grain Size, μm	Silicate-Metal Size Ratio	Status of Metal
1	0.05	149-250	425-600	2.6 ± 0.8	mixing
2	0.05	149-250	300-425	1.8 ± 0.5	jetsam
3	0.07	53-74	425-600	8.1 ± 1.6	flotsam
4	0.07	74-105	300-425	4.1 ± 0.8	flotsam
5	0.08	105-149	250-300	2.2 ± 0.4	jetsam
6	0.09	74-105	425-600	5.7 ± 1.1	flotsam
7	0.09	105-149	425-600	4.0 ± 0.8	flotsam
8	0.10	149-250	425-600	2.6 ± 0.8	mixing
9	0.10	149-250	600-710	3.3 ± 1.0	mixing
10	0.13	53-74	300-425	5.7 ± 1.1	flotsam
11	0.15	53-74	425-600	8.1 ± 1.6	flotsam
12	0.16	105-149	250-300	2.2 ± 0.4	jetsam
13	0.19	74-105	300-425	4.1 ± 0.8	flotsam
14	0.19	105-149	250-500	3.0 ± 1.2	mixing
15	0.21	74-105	425-600	5.7 ± 1.1	flotsam
16	0.22	149-250	149-250	1.0 ± 0.4	jetsam
17	0.26	53-74	300-425	5.7 ± 1.1	flotsam
18	0.32	149-250	425-600	2.6 ± 0.8	jetsam
19	0.32	74-105	425-600	5.7 ± 1.1	flotsam
20	0.38	53-74	300-425	5.7 ± 1.1	mixing
21	0.39	105-149	300-425	2.9 ± 0.6	jetsam
22	0.41	74-105	300-425	4.1 ± 0.8	mixing
23	0.46	53-74	425-600	8.1 ± 1.6	flotsam
24	0.47	105-149	250-300	2.2 ± 0.4	jetsam
25	0.50	53-74	300-425	5.7 ± 1.1	mixing

size ratio ≥ 4 and the iron fraction is <25 vol.% of the bed. At higher iron volume fractions the bed becomes primarily well mixed owing to the reduced amount of available pore space for the iron grains to travel through and since the addition of fines reduces the overall minimum fluidization velocity for the entire bed [*Rincón et al.*, 1994]. Mixing is defined by an index of $0.95<M<1.05$ [*Chiba et al.*, 1980]. The behavior of iron as jetsam is largely insensitive to its bed abundance. Diameter ratios <2.5 result in beds with iron-depleted surfaces. Table 3 summarizes the quartz and iron grain properties in each of the fluidization runs shown in Figure 6.

Until now the discussion has centered on the readily achievable metal-silicate fractionations that resulted from the large size difference between quartz and iron grains. Fluidization also results in the size sorting of individual components. Figure 7 shows the segregation tendency of quartz in a fluidization run involving a chondritic-like mixture of particulates. The largest quartz grains settled to the bottom of the bed, while the smaller grains remained fluidized longer during the terminal stages of degassing and traveled upward with the gas flow. The result is a segregation in quartz sizes with depth that may represent the effects of fluidization on

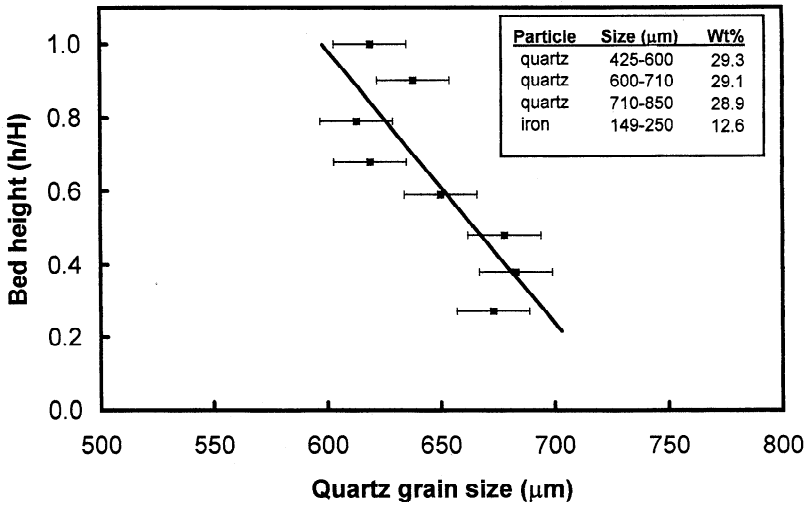

Figure 7. Size sorting of quartz grains (425-850 μm) from a fluidization run. Sorting followed the expected trend of the largest particles sinking in the bed, while the smaller quartz grains concentrated closer to the bed surface. Error bars are two sigma standard deviation of the mean for repeatability in grain size measurement.

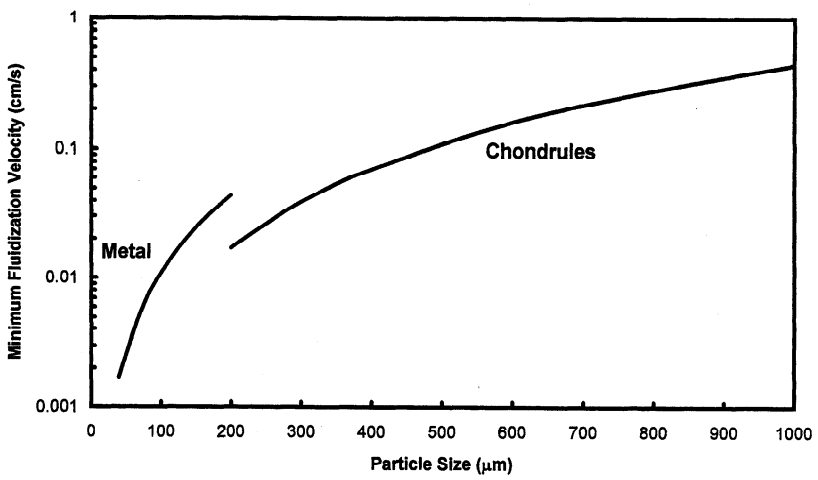

Figure 8. Minimum fluidization velocity for a 100 km diameter asteroid. The minimum fluidization velocity was calculated from (A4) and is the minimum escaping gas velocity needed to cause fluidization. Parameters and values used in the equations are listed in Table A1. Chondrule sizes larger than 300 μm require higher gas flow rates than metal grains to become fluidized. Experiments suggest that the more easily fluidized metal grains should be carried upward in a fluidized regolith, while chondrules would gradually sink. Minimum fluidization velocity varies approximately with asteroid size. Thus a 200 km diameter asteroid would require gas flow rates twice those in this figure.

chondrule sorting. Even in the absence of iron grains, similar quartz sorting is observed.

6. Fluidization on Chondritic Parent Bodies

The potential for fluidized metal-silicate fractionations on chondritic parent bodies requires only one major assumption, that these bodies were initially volatile-rich (we generally assume H_2O). This assumption is not unreasonable, since approximately one-third of all asteroids show spectral absorption features similar to carbonaceous chondrites [*Tholen*, 1989; *Gaffey et al.*, 1993]. *Barucci et al.* [1998] found that 70% of the asteroids studied in their C-class asteroid survey had surfaces that appeared aqueously altered. The CI and CM chondrites contain 17 and 10 wt% water [*Jarosewich*, 1990], respectively, suggesting that the parent bodies of these chondrites were water-rich. Aqueous alteration products have also been observed in CV and CO [*Zolensky and McSween*, 1988] and the unmetamorphosed ordinary chondrites [*Hutchison et al.*, 1987; *Alexander et al.*, 1989]. Other volatiles may also be released at higher metamorphic temperatures. *Muenow et al.* [1995] found significant amounts of CO, CO_2, and Cl were released from ordinary chondrites at temperatures >600°C, sufficient to obtain pyroclastic volcanism on differentiated asteroids.

The duration of parent body degassing depends on the permeability and thickness of the regolith and the nature of the heat source. *Huang et al.* [1996a] calculated the gas flow rates of water released during impact and ^{26}Al heating and found both mechanisms were sufficient for fluidization and would result in dehydration of a 2.5 km thick regolith in a few months to a few years. Degassing on this timescale is more than sufficient, since fluidized segregation on the laboratory scale generally operates on the order of seconds to minutes.

Figure 8 shows the minimum gas velocities (v_{mf}) needed to obtain fluidization on a 100 km meteorite parent body. Experiments with chondritic analogs described earlier suggest that maximum sorting takes place at gas velocities just below the v_{mf} of the larger particle. In a fluidized regolith the heavier grains will sink (jetsam), while the lighter grains will travel upward (flotsam) with the escaping gas flow. Since the minimum fluidization velocity of a given particle varies with its weight, Figure 8 shows that all chondrites with mean chondrule sizes > 300 μm would behave as jetsam. In fact, all chondritic classes appear to have mean chondrule v_{mf} > mean metal v_{mf}, which implies that in chondritic meteorite parent bodies, chondrules behave as jetsam while metal grains are flotsam.

Of primary importance in the fluidization model is its ability to explain the observed metal-silicate fractionations and apparent chondrule sorting in chondrites. The depletion of Fe relative to Si (Figure 1) is unique to each chondritic class and may well reflect heterogeneous distribution of Fe in the solar

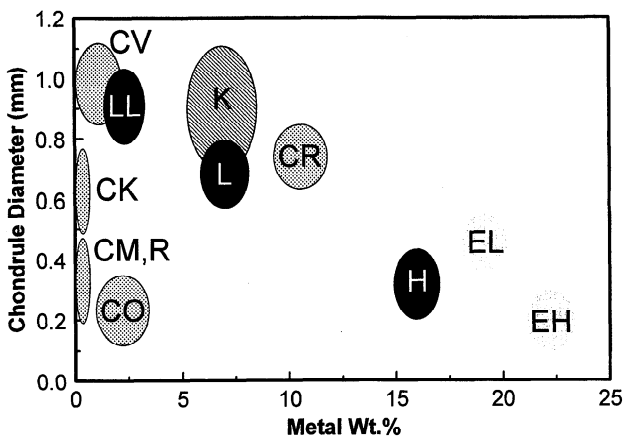

Figure 9. Chondrule size versus metal abundance in chondritic meteorites. Mean chondrule size tends to decrease with increasing metal abundance in all but the most highly oxidized chondrites. Data from Table 1, *Kallemeyn et al.* [1991, 1994, 1996], and *Weisberg et al.* [1996].

nebula; however, this alone fails to explain the Fe/Si differences found among ordinary and enstatite chondrites whose members presumably formed in close proximity to each other. Fluidization of these parent bodies could segregate metal grains into a thin zone near the surface or several zones if degassing was episodic during accretion. Occurring simultaneously with metal-silicate fractionation would be chondrule sorting in which the smallest chondrules would be carried upward in the gas flow along with the metal. The fluidization model predicts that meteorites with the smallest mean chondrule sizes should be found in association with abundant metal grains. Figure 9 is a plot of chondrule diameter versus metal wt% for the major chondrite classes and demonstrates the inverse correlation as would be expected from fluidization. The highly oxidized groups do not follow the inverse correlation trend due to their lack of metal but were still chondrule sorted.

7. Carbonaceous Chondrites

The carbonaceous chondrites are the most highly oxidized and contain the greatest abundance of volatiles of all the chondritic meteorites. All four of the major groups (CV, CO, CM, and CI) contain evidence for aqueous alteration presumably on their parent bodies [*Zolensky and McSween*, 1988; *Krot et al.*, 1998], although some aqueous alteration may have occurred before final agglomeration [*Bischoff*, 1998]. The CI and CM chondrites contain substantial amounts of hydrated silicates, suggesting that the heating mechanism was insufficient in dehydrating the source bodies. Carbonaceous chondrites can be dehydrated by heating between 600 and 900 K, with up to 95% by volume of the evolved gases being H_2O, CO, and CO_2 [*Lebofsky et al.*, 1989]. Therefore modest heating by radiogenic nuclides or impact would easily liberate the trapped gases. The lack of metal grains prevented significant metal-silicate fractionations in CI and CM, although CM did undergo chondrule sorting. The CV and CO groups are more dehydrated and contain small amounts of FeNi metal. The presence of metal means that fluidization could segregate these components more efficiently, leading to the greater fractionation in Fe/Si than that observed in CM and CI. All the carbonaceous groups also appear to have undergone chondrule sorting, except for CI, which lack chondrules. The range for average chondrule diameter, however, varies widely, from 0.25 mm for CO to 1.0 mm for CV. This could be the result of different chondrule size populations resulting from the formation of chondrules on parent body surfaces [*Symes et al.*, 1998] or accretion to their respective parent bodies [*Liffman and Brown*, 1996]. We have previously speculated that impact formation of chondrules could also be the driving force behind volatile depletion in chondrites [*Sears and Akridge*, 1998]. This idea is supported by the apparent reduction in FeO that accompanied chondrule formation [*Huang et al.*, 1996b] and the presence of chondrule-like objects produced by very large impacts on the Moon [*Symes et al.*, 1998; *Ruzicka et al.*, 1998a,b].

8. Enstatite Chondrites

The enstatite chondrites, EH and EL, are the most highly reduced and may best represent the concept of fluidization. Although both classes contain unique size distributions for chondrules and metal grains, the size ratio of 5.5 is similar for both classes. Sorting for both classes had a remarkably similar efficiency. The two classes are mainly subdivided based on their

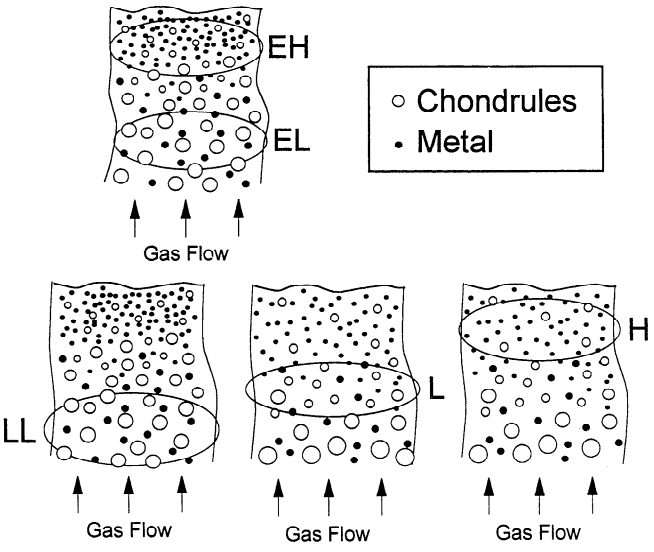

Figure 10. Possible parent body sorting scenarios. Experimental data suggest that enstatite chondrites could be derived from a single sorting event which segregated chondrules and metal. Siderophile abundance and chondrule and metal grain sizes are consistent with this scenario. Chemical and particulate size data indicate fluidization may have been less efficient for the ordinary chondrites. Although formation of ordinary chondrites in a single column is not ruled out, it appears more likely that H, L, and LL derived from different locations on single or multiple parent bodies.

iron content [*Sears et al.*, 1982], with EH being enriched in siderophile elements. The fact that they are currently volatile depleted does not, however, preclude an initially substantial volatile content. If fluidization was occurring during accretion, subsequent radioactive heating lasting millions of years could have erased any short-lived aqueous alteration effects while preserving the stratigraphic sorting within the body. We would also not rule out fluidization by other volatiles such as CO, N_2, and Cl [*Muenow et al.*, 1992]. *Wilson and Keil* [1991] argued that the aubrite parent body (expected to have the same precursor composition as enstatite chondrites) may have contained melts with sufficient volatiles to eject material at speeds in excess of the asteroid's escape velocity upon eruption.

We suggest that both EH and EL may have originated from separate locations within a single parent body (Figure 10). Fluidization would carry metal grains and smaller chondrules upward toward the surface of the body, resulting in deeper regions that are relatively metal-poor with larger chondrules. These deeper regions would have properties similar to EL, with the metal-rich EH regions lying closer to the surface. Thus EH and EL chondrites may be merely reflecting pre-impact ejection depth within the parent body. This could explain the unique Fe/Si abundance [*Sears and Dodd*, 1988] and the widely differing cooling rates between the two classes [*Zhang et al.*, 1996]. The more rapid cooling of EH relative to EL may reflect postmetamorphism burial depth in a thick regolith. *Keil* [1989] argued that EH and EL must originate from separate parent bodies based on the abundance of monomict breccias (25%) and bulk compositional differences. The breccias are monomict in the sense that there appears to be no mixing of EH and EL clasts

within a single centimeter-sized meteorite. Keil, however, was not thinking in terms of mass movement of material on the parent body. The upward movement of siderophiles created the two classes and is responsible for the resulting bulk chemical differences. Fragmental breccias containing only a single enstatite class is expected in our fluidization model, since many if not all enstatite chondrites formed after segregation of material in a regolith. The nearly identical oxygen isotope values for EH and EL [*Clayton et al.*, 1984] also indicate either a single source body or two parent bodies that accreted in close proximity in the nebula.

9. Ordinary Chondrites

The chondrule sizes in H, L, and LL have unique distributions and suggest that some type of sorting must have occurred. However, the size distribution of metal grains is very similar in each class [*Dodd,* 1976] and appears to be poorly sorted. We believe that *Dodd* [1976] was measuring all metal grain sizes including those attached to chondrule rims. *Benoit et al.* [1998] remeasured the chondrule and metal grain sizes in Sharps (H3.4) and found similar chondrule sizes but a significantly smaller average metal grain size than those reported by Dodd. The chondrule to metal size ratio of Benoit et al. for Sharps is 4.9, well within the field for metal grains to behave as flotsam (Figure 11). If these new data are respresentative for all H chondrites, then the ordinary chondrites may have experienced similar degrees of fluidization and sorting. Much like the enstatite chondrites, the metal-rich H appear to be samples from close to the surface, while L and LL represent samples derived from greater depth, although oxygen isotopes [*Clayton et al.*, 1991] and other data suggest that it is less likely the three ordinary chondrite classes derived from the same parent body (Figure 10).

If chondritic parent bodies accreted volatile-rich materials, then extensive degassing has occurred either through impact or interior heating. *Akridge et al.* [1998] modeled the thermal metamorphism of the H chondrite parent body by the decay of ^{26}Al and found a steep temperature gradient near the surface caused by the effective insulation provided by the overlying regolith. The peak temperatures and cooling rates of all H chondrites match the calculated properties of the regolith environment in the Akridge et al. model. If H chondrites (and other chondrites?) originated in a regolith, then parent body degassing would unavoidably cause size and density segregation of the sort described here. Global heating by ^{26}Al or any other mechanism would result in relatively slow release of trapped volatiles and hydrated silicates, leading to smooth fluidization over a large fraction of the body. Heating by impact is a rapid and highly localized process that would liberate trapped volatiles near the surface, causing fluidized size sorting on a smaller scale. Channeling or venting can occur as the liberated gas coallesces and is expected to result from both rapid and slow duration heating events.

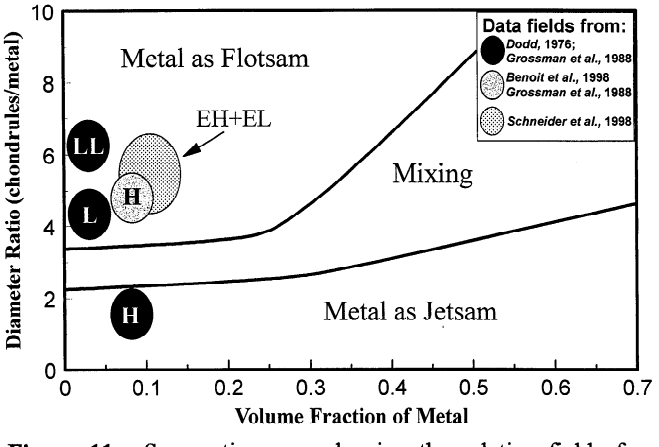

Figure 11. Segregation map showing the relative fields for ordinary and enstatite chondrites. Only H chondrites appear to metal behaving as jetsam. *Benoit et al.* [1998], however, found smaller metal grain sizes in Sharps (H3.4) than *Dodd* [1976], which may indicate that even H chondrites fall into the metal as flotsam region.

One inescapable result of fluidization is the formation of a complex stratigraphy. The sorting of metal and chondrules, and presumably other particles of intermediate sizes and densities such as sulfides, would result in metal-rich and metal-poor regions. Thus asteroids are probably not the relatively homogeneous bodies differing only in petrographic type from region to region as is generally thought. Enriching the surface with metal grains may help explain the mismatch between the spectral characteristics of ordinary chondrites and asteroids [*Gaffey et al.*, 1993]. The surfaces of the most likely ordinary chondrite parent bodies appear to be enriched in metal, and numerous explanations have been suggested to explain this difference, including space weathering [*Chapman,* 1996] and impact alteration of the regolith [*Britt and Pieters*, 1991]. The current fluidization model delivers metal to the near-surface regions that is probably thoroughly mixed through the upper regolith by later small impacts.

10. Conclusions

Experiments using quartz and iron grains as chondritic analogs have shown rapid segregation of the two components, with iron grains traveling upward with the gas flow while quartz grains sink in a fluidized bed. The result is a dramatic metal-silicate fractionation between the top and bottom of the fluidized layers. Applying these results to the chondritic meteorites indicates that similar types of fluidized sorting may be responsible for the observed metal-silicate fractionation and chondrule size distributions found in the enstatite, ordinary, and carbonaceous chondrites.

Our experiments were conducted using Earth's gravity and at atmospheric pressure. These results should be tested at conditions more appropriate for asteroids such as 0.01 *g* and low pressures. No previous work has been conducted concerning fluidized size-sorting in low-gravity environments, but *Miller and King* [1966] have experimentally examined fluidization under low pressure. Their pre-lunar landing work looked at the potential for creating lunar craters by volatile outgassing and did not consider the possibility of particulate sorting. *Mills* [1969] was also able to recreate many lunar crater morphological features by fluidizing a lunar-like regolith.

It seems probable that many if not most asteroids initially accreted with substantial volatile inventories. We suspect that the release of these volatiles during parent body heating created dynamic regoliths in which particle movement would be governed by the escaping gas flow and their physical properties. Initially, gas velocities would be too high for efficient sorting, but the terminal stages of degassing would create ideal conditions for segregation of metal from chondrules.

Appendix

A1. Fluidization

Fluidization occurs whenever a gas is passed upward through a bed of cohesionless particles at a rate great enough for the gas drag to balance the force of gravitational attraction [*Kunii and Levenspiel,* 1991]. The lowest gas flow rate at which this occurs is referred to as the minimum fluidization velocity. Upon reaching the minimum fluidization velocity, the bed begins to expand and the particles attain fluid-like characteristics. Bubbling within the bed often occurs, since the interstitial gas begins to coalesce before reaching the bed surface [*Kunii and Levenspiel,* 1991]. Particles are free to move about the bed, with larger and denser particles tending to sink and smaller and lighter particles rising. The component that ultimately sinks is referred to as "jetsam," and the component that ultimately floats as "flotsam." Segregation of bed components can occur whenever rising bubbles temporarily disturb a localized region. As a bubble rises, the jetsam and flotsam are drawn into its wake, with the jetsam settling out more quickly. The result is a net downflow of jetsam while flotsam travels upward in the bed until an equilibrium is reached where segregation tendencies are balanced by localized particle mixing [*Gibilaro and Rowe,* 1974; *Rowe and Nienow,* 1976]. The lack of bubbling below the minimum fluidization velocity prevents bed segregation because interparticle forces restrict movement within the bed. At high gas flow rates the bed will become turbulent with particle mixing predominating over segregation.

The minimum fluidization velocity (v_{mf}) for a system can be determined either empirically or through predictive equations. Measuring the pressure drop across a bed while the gas flow (v) is steadily increased will define a point at which the pressure differential remains constant (or even drops), since at gas flows above v_{mf} the bed can deform easily with little resistance (Figure 4). Thus v_{mf} is found by locating the intersection of two extrapolated lines through the pressure drop data [*Kunii and Levenspiel,* 1991]. *Rincón et al.* [1994] have suggested that the v_{mf} of a binary mixture can be deduced provided the pressure drop data for each of the components is known. The gas flow required to begin minimum fluidization can also be calculated theoretically using the *Ergun* [1952] equation:

Table A1. Parameters Used in the Calculations

Symbol	Meaning	Value	Unit
μ	viscosity of water vapor	1-2 x 10^{-4}	g cm^{-1} s^{-1}
ϕ	sphericity	0.66-0.9	
ε	void fraction	0.4-0.6	
ρ_s	density of solid	2.6-8	g cm^{-3}
ρ_g	density of gas - water vapor	2-6 x 10^{-4}	g cm^{-3}
g_a	acceleration of gravity on asteroid	0.8-8	cm s^{-2}
g_e	acceleration of gravity on earth	980	cm s^{-2}
d	diameter of particle	40-1000	μm

$$\frac{1.75R_e^2}{\varepsilon^3\phi}+\frac{150(1-\varepsilon)R_e}{\varepsilon^3\phi^2}=\frac{d^3\rho_g(\rho_s-\rho_g)g}{\mu^2} \qquad \text{(A1)}$$

where ε is the void fraction under minimum flow conditions, ϕ the sphericity of the particle, d the particle diameter, ρ_g and ρ_s the densities of the gas and solid, g the gravitational acceleration, μ the viscosity of gas, and R_e the Reynolds number. The Reynolds number depends primarily on the minimum gas flow rate and particle diameter:

$$R_e=\frac{dv_{mf}\rho_g}{\mu} \qquad \text{(A2)}$$

In cases where ε and ϕ are poorly known, *Wen and Yu* [1966a,b] found that

$$\frac{dv_{mf}\rho_g}{\mu}=\left[33.7^2+0.0408\frac{d^3\rho_g(\rho_s-\rho_g)g}{\mu^2}\right]^{0.5}-33.7 \qquad \text{(A3)}$$

approximates the gas flow behavior through packed beds. At low R_e, (A3) simplifies to

$$v_{mf}=\frac{d^2(\rho_s-\rho_g)g}{1650\mu} \qquad R_e<20 \qquad \text{(A4)}$$

while at high R_e,

$$v_{mf}=\left[\frac{d(\rho_s-\rho_g)g}{24.5\rho_g}\right]^{0.5} \qquad R_e>1000. \qquad \text{(A5)}$$

For chondrules and chondritic metal under low-gravity conditions (10^{-3}-10^{-2} g_e) the gas flow required for minimum fluidization is sufficiently low so that R_e <<20. Parameters and values used in the equations are listed in Table A1.

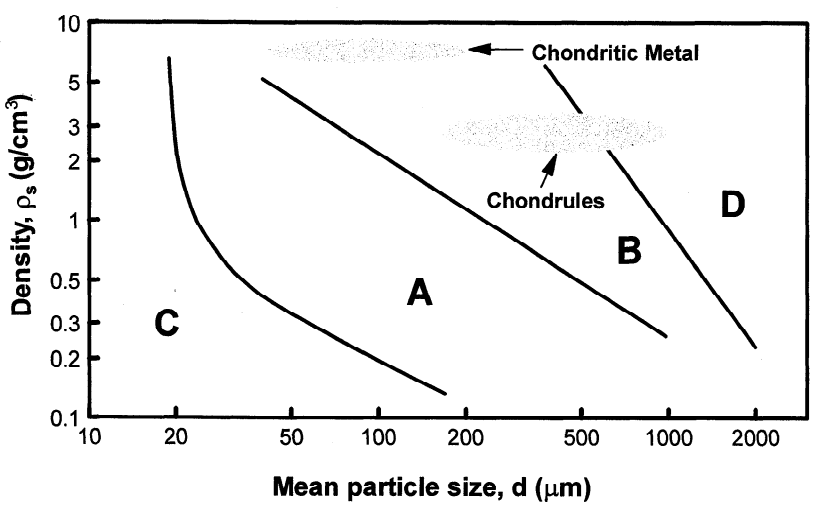

Figure A1. Geldart classification of particles fluidized in ambient air. Particulates behave in one of four groups according to their density and mean particle size (see text for description of each zone). Chondritic metal and most chondrules behave like Geldart B solids which can be easily fluidized.

A2. Particle Classification

The behavior of fluidized particles of widely varying densities and sizes falls into four distinct groups [*Geldart*, 1973]. The Geldart classification of particles separates these groups (Figure A1) by virture of their observed bed properties and bubble behavior. *Kunii and Levenspiel* [1991] summarized the distinctive properties of each group as follows.

Group A: aeratable. Fluidization is smooth and occurs easily. Bed expansion occurs before the onset of bubbling. Gas bubbles split and coalesce easily and rise more quickly than the rest of the gas. Circulation of bed solids is more pronounced than for other groups.

Group B: sandlike. These solids also fluidize easily with bubbles forming immediately upon reaching v_{mf}. Bubbles grow linearly with height within the bed forming large bubbles at the surface. Circulation of solids increases with vigorous bubbling.

Group C: cohesive. These very fine powders are difficult to fluidize due to electostatic forces between grains predominating over gas action. Particles tend to rise in mass or plugs and the gas may sometimes carve out channels.

Group D: spoutable. Large particles tend to behave erratically, causing severe channeling. Bubbles coalesce quickly and grow to a large size but rise more slowly than the rest of the gas. Spouting is common whereby solids can be transported to the top of the bed by individual bubbles. Downward movement occurs with solids filling the voids left by spouted bubbles.

The regions for meteoritic chondrules and metal are plotted in Figure A1 to show the expected bed behavior for these materials. Both components fall largely into the sandlike category and should be readily fluidized. Even the largest chondrules which fall into the Geldart D region would be readily fluidized when mixed in a bed of smaller particles such as matrix, metal and sulfide grains, and fragmented chondrules.

Acknowledgments. We would like to thank Alex Ruzicka and Tim McCoy for insightful and constructive reviews. We would also like to thank W. Roy Penney, Chemical Engineering Department, University of Arkansas, for advice and the use of equipment.

References

Akridge, G., P. H. Benoit, and D. W. G. Sears, Regolith and megaregolith formation of H-chondrites: Thermal constraints on the parent body, *Icarus, 132*, 185-195, 1998.

Alexander, C. M. O., R. Hutchinson, and D. J. Barber, Origin of chondrule rims and interchondrule matrices in unequilibrated ordinary chondrites, *Earth Planet. Sci. Lett., 95*, 187-207, 1989.

Barucci, M. A., A. Doressoundiram, M. Fulchignoni, M. Florczak, M. Lazzarin, C. Angeli, and D. Lazzaro, Search for aqueously altered materials on asteroids, *Icarus, 132*, 388-396, 1998.

Benoit, P. H., G. Akridge, and D. W. G. Sears, Size sorting of metal, sulfide, and chondrules in Sharps (H3.4) (abstract 1457), *Lunar Planet. Sci., XXIX*, [CD-ROM], 1998.

Bischoff, A., Aqueous alteration of carbonaccous chondrites: Evidence for preaccretionary alteration-A review, *Meteorit. Planet. Sci., 33*, 1113-1122, 1998.

Britt, D. T., and C. M. Pieters, Darkening in gas-rich ordinary chondrites: Spectral modelling and implications for the regoliths of ordinary chondrite parent bodies (abstract), *Lunar Planet. Sci., XXII*, 141-142, 1991.

Cameron, A. G. W., The first ten million years in the solar nebula, *Meteoritics, 30*, 133-161, 1995.

Carey, S. N., Transport and deposition of tephra by pyroclastic flows and surges, in *Sedimentation in Volcanic Settings, SEPM Spec. Publ. 45*, pp. 39-57, Soc. of Econ. Paleontol. and Mineral., Tulsa, Okla., 1991.

Chapman, C., S-type asteroids, ordinary chondrites, and space weathering: The evidence from *Galileo*'s fly-bys of Gaspra and Ida, *Meteorit. Planet. Sci., 31*, 699-725, 1996.

Chiba, S., A. W. Nienow, T. Chiba, and H. Kobayashi, Fluidised binary mixtures in which the denser component may be flotsam, *Powder Technol., 26*, 1-10, 1980.

Clayton, D. D., Chemical and isotopic fractionation by grain size seperates, *Earth Planet. Sci. Lett., 47*, 199-210, 1980.

Clayton, R. N., N. Onuma, and T. K. Mayeda, A classification of meteorites based on oxygen isotopes, *Earth Planet. Sci. Lett., 30*, 10-18, 1976.

Clayton, R. N., T. K. Mayeda, and A. E. Rubin, Oxygen isotopic compositions of enstatite chondrites and aubrites, *Proc. Lunar Planet. Sci. Conf.*, Part 1, *J. Geophys. Res., 89*, suppl., *15*, C245-C249, 1984.

Clayton, R. N., T. K. Mayeda, J. N. Goswami, and E. J. Olsen, Oxygen isotope studies of ordinary chondrites, *Geochim. Cosmochim. Acta, 55*, 2317-2337, 1991.

Delebarre, A. B., A. Pavinato, and J. C. Leroy, Fluidization and mixing of solids distributed in size and density, *Powder Technol., 80*, 227-233, 1994.

Dodd, R. T., Accretion of the ordinary chondrites, *Earth Planet. Sci. Lett., 28*, 281-291, 1976.

Donn, B., and G. W. Sears, Planets and comets: Role of crystal growth in their formation, *Science, 140*, 1208-1211, 1963.

Ergun, S., Fluid flow through packed columns, *Chem. Eng. Prog., 48*, 89-94, 1952.

Gaffey, M. J., T. H. Burbine, and R. P. Binzel, Asteroid spectroscopy: Progress and perspectives, *Meteoritics, 28*, 161-187, 1993.

Geldart, D., Types of gas fluidization, *Powder Technol., 7*, 285-292, 1973.

Gibilaro, L. G., and P. N. Rowe, A model for a segregating gas fluidised bed, *Chem. Eng. Sci., 29*, 1403-1412, 1974.

Grossman, J. N., A. E. Rubin, H. Nagahara, and E. A. King, Properties of chondrules, in *Meteorites and the Early Solar System*, edited by J. F. Kerridge and M. S. Matthews, pp. 619-659, Univ. of Ariz. Press, Tucson, 1988.

Haack, H., and E. R. D. Scott, Nebula formation of the H, L, and LL bodies from a single batch of chondritic materials (abstract), *Meteoritics, 28*, 358-359, 1993.

Hoblitt, R. P., C. D. Miller, and J. W. Vallance, Origin and stratigraphy of the deposit produced by the May 18 directed blast, in *The 1980 Eruptions of Mount St. Helens, Washington*, edited by P. W. Lipman and D. R. Mullineaux, *U. S. Geol. Surv. Prof. Pap. 1250*, 401-419, 1981.

Huang, S., G. Akridge, and D. W. G. Sears, Metal-silicate fractionation in the surface dust layers of accreting planetesimals: Implications for the formation of ordinary chondrites and the nature of asteroid surfaces, *J. Geophys. Res., 101*, 29,373-29,385, 1996a.

Huang, S., J. Lu, M. Prinz, M. K. Weisberg, P. H. Benoit, and D. W. G. Sears, Chondrules: Their diversity and the role of open-system processes during their formation, *Icarus, 122*, 316-346, 1996b.

Hughes, D. W., A disaggregation and thin section analysis of the size and mass distribution of the chondrules in the Bjurbole and Chainpur meteorites, *Earth Planet. Sci. Lett., 38*, 391-400, 1978.

Hutcheon, I. D., G. R. Huss, and G. J. Wasserburg, A search for ^{26}Al in chondrites: Chondrule formation time scales (abstract), *Lunar Planet. Sci., XXV*, 587-588, 1994.

Hutchison, R., C. M. O. Alexander, and D. J. Barber, The Semarkona meteorite: First recorded occurrence of smectite in an ordinary chondrite, and its implications, *Geochim. Cosmochim. Acta, 51*, 1875-1882, 1987.

Jarosewich, E., Chemical analyses of meteorites: A compilation of stony and iron meteorite analyses, *Meteoritics, 25*, 323-337, 1990.

Kallemeyn, G. W., A. E. Rubin, and J. T. Wasson, The compositional classification of chondrites: V. The Karoonda (CK) group of carbonaceous chondrites, *Geochim. Cosmochim. Acta, 55*, 881-892, 1991.

Kallemeyn, G. W., A. E. Rubin, and J. T. Wasson, The compositional classification of chondrites: VI. The CR carbonaceous chondrite group, *Geochim. Cosmochim. Acta, 58*, 2873-2888, 1994.

Kallemeyn, G. W., A. E. Rubin, and J. T. Wasson, The compositional classification of chondrites: VII. The R chondrite group, *Geochim. Cosmochim. Acta, 60*, 2243-2256, 1996.

Keil, K., Enstatite meteorites and their parent bodies, *Meteoritics, 24*, 195-208, 1989.

King, T. V. V., and E. A. King, Size-frequency distributions of fluid drop chondrules in ordinary chondrites, *Meteoritics, 14*, 91-96, 1979.

Krot, A. N., M. I. Petaev, E. R. D. Scott, B. G. Choi, M. E. Zolensky, and K. Keil, Progressive alteration in CV3 chondrites: More evidence for asteroidal alteration, *Meteorit. Planet. Sci., 33*, 1065-1085, 1998.

Kunii, D., and O. Levenspiel, *Fluidization Engineering*, 2nd ed., Butterworth-Heinemann, Newton, Mass., 1991.

Larimer, J. W., and E. Anders, Chemical fractionation in meteorites, III, Major element fractions in chondrites, *Geochim. Cosmochim. Acta, 34*, 367-387, 1970.

Larimer, J. W., and J. T. Wasson, Siderophile element fractionation, in *Meteorites and the Early Solar System*, edited by J. F. Kerridge and M. S. Matthews, pp. 416-435, Univ. of Ariz. Press, Tucson, 1988.

Lebofsky, L. A., T. D. Jones, and E. Herbert, Asteroid volatile inventories, in Origin and Evolution of Planetary and Satellite Atmospheres, edited by S. K. Atreya, J. B. Pollack, and M. S. Matthews, pp. 192-229, Univ. of Ariz. Press, Tucson, 1989.

Liffman, K., and M. J. I. Brown, The motion and size sorting of particles ejected from a protostellar accretion disk, *Icarus, 116*, 275-290, 1995.

Liffman, K., and M. J. I. Brown, The protostellar jet model of chondrule formation, in *Chondrules and the Protoplanetary Disk*, edited by R. H. Hewins, R. H. Jones, and E. R. D. Scott, pp. 285-302, Cambridge Univ. Press, New York, 1996.

Martin, P. M., and A. A. Mills, Size and shape of chondrules in the Bjurbole and Chainpur meteorites, *Earth Planet. Sci. Lett., 33*, 239-248, 1976.

Martin, P. M., and A. A. Mills, Size and shape of near-spherical Allegan chondrules, *Earth Planet. Sci. Lett., 38*, 385-390, 1978.

Miller, G. H., and I. R. King, An experimental study of fluidization processes under lunar conditions, *NASA Contract. Rep., 627*, 92 pp., 1966.

Mills, A. A., Fluidization phenomena and possible implications for the origin of lunar craters, *Nature, 224*, 863-866, 1969.

Muenow, D. W., K. Keil, and L. Wilson, High-temperature mass spectrometric degassing of enstatite chondrites: Implications for pyroclastic volcanism on the aubrite parent body, *Geochim. Cosmochim. Acta, 56*, 4267-4280, 1992.

Muenow, D. W., K. Keil, and T. J. McCoy, Volatiles in unequilibrated ordinary chondrites: Abundances, sources and implications for explosive volcanism on differentiated asteroids, *Meteoritics, 30*, 639-645, 1995.

Newsom, H. E., Metal-silicate fractionation in the solar nebula (abstract), *Lunar Planet. Sci., XXVI*, 1043-1044, 1995.

Newsom, H. E., G. Graup, T. Sewards, and K. Keil, Fluidization and hydrothermal alteration of the suevite deposit at the Ries Crater, West Germany, and implications for Mars, *J. Geophys. Res., 91(B13)*, 239-251, 1986.

Nienow, A. W., P. N. Rowe, and T. Chiba, Mixing and segregation of a small proportion of large particles in gas fluidized beds of considerably smaller ones, *AIChE Symp. Ser., 74(176)*, 45-53, 1978.

Orowan, E., Density of the moon and nucleation of planets, *Nature, 222*, 867, 1969.

Podosek, F. A., and P. Cassen, Theoretical, observational, and isotopic estimates of the lifetime of the solar nebula, *Meteoritics, 29*, 6-25, 1994.

Rincón, J., J. Guardiola, A. Romero, and G. Ramos, Predicting the minimum fluidization velocity of multicomponent systems, *J. Chem. Eng. Jpn., 27*, 177-181, 1994.

Rowe, P. N., and A. N. Nienow, Particle mixing and segregation in gas fluidised beds. A review, *Powder Technol., 15*, 141-147, 1976.

Rowe, P. N., A. W. Nienow, and A. J. Agbim, The mechanisms by which particles segregate in gas fluidised beds - Binary systems of near-spherical particles, *Trans. Inst. Chem. Eng., 50*, 310-323, 1972a.

Rowe, P. N., A. W. Nienow, and A. J. Agbim, A preliminary quantitative study of particle segregation in gas fluidised beds - Binary systems of near spherical particles, *Trans. Inst. Chem. Eng., 50*, 324-333, 1972b.

Rubin, A. E., and K. Keil, Size-distributions of chondrule types in the Inman and Allan Hills A77011 L3 chondrites, *Meteoritics, 19*, 135-143, 1984.

Ruzicka, A., G. A. Snyder, A. D. Patchen, and L. A. Taylor, Lunar chondrules: Impact-melting of highland lithologies (abstract 1434), *Lunar Planet. Sci., XXIX*, [CD-ROM], 1998a.

Ruzicka, A., G. A. Snyder, A. D. Patchen, and L. A. Taylor, Lunar chondrule petrography and mineral chemistry: Rims, relict grains, and metasomatism (abstract 1436), *Lunar Planet. Sci., XXIX*, [CD-ROM], 1998b.

Schneider, D. M., D. G. Akridge, and D. W. G. Sears, Size distribution of metal grains and chondrules in enstatite chondrites (abstract), *Meteorit. Planet. Sci., 33*, A136-A137, 1998.

Scott, E. R. D., and H. Haack, Chemical fractionation in chondrites by aerodynamic sorting of chondritic materials (abstract), *Meteoritics, 28*, 434, 1993.

Sears, D. W. G., and G. Akridge, Nebular or parent body alteration of chondritic material: Neither or both?, *Meteorit. Planet. Sci., 33*, 1157-1167, 1998.

Sears, D. W. G., and R. T. Dodd, Overview and classification of meteorites, in *Meteorites and the Early Solar System*, edited by J. F. Kerridge and M. S. Matthews, pp. 3-31, Univ. of Ariz. Press, Tucson, 1988.

Sears, D. W., G. W. Kallemeyn, and J. T. Wasson, The compositional classification of chondrites: II The enstatite chondrite groups, *Geochim. Cosmochim. Acta, 46*, 597-608, 1982.

Sears, D. W. G., S. Huang, and P. H. Benoit, Formation of chondrules in a thick dynamic regolith (abstract), *Meteoritics, 29*, 531, 1994.

Sears, D. W. G., S. Huang, and P. H. Benoit, The formation of chondrules (abstract), *Lunar Planet. Sci., XXVI*, 1263-1264, 1995.

Shu, F. H., H. Shang, and T. Lee, Toward an astrophysical theory of chondrites, *Science, 271*, 1545-1552, 1996.

Skinner, W. R., and J. M. Leenhouts, Size distributions and aerodynamic equivalence of metal chondrules and silicate chondrules in Acfer 059 (abstract), *Lunar Planet. Sci., XXIV*, 1315-1316, 1993.

Swindle, T. D., A. M. Davis, C. M. Hohenberg, G. J. MacPherson, and L. E. Nyquist, Formation times of chondrules and Ca-Al-rich inclusions: Constraints from short-lived radionuclides, in *Chondrules and the Protoplanetary Disk*, edited by R. H. Hewins, R. H. Jones, and E. R. D. Scott, pp. 77-86, Cambridge Univ. Press, New York, 1996.

Symes, S. J. K., D. W. G. Sears, D. G. Akridge, S. Huang, and P. H. Benoit, The crystalline lunar spherules: Their formation and implications for the origin of meteoritic chondrules, *Meteorit. Planet. Sci., 33*, 13-29, 1998.

Tholen, D. J., Asteroid taxonomic classifications, in *Asteroids II*, edited by R. P. Binzel, T. Gehrels, and M. S. Matthews, pp. 1139-1150, Univ. of Ariz. Press, Tucson, 1989.

Urey, H. C., Criticism to Dr. B. Mason's paper on "Origin of Meteorites," *J. Geophys. Res., 66*, 1988-1991, 1961.

Wasson, J. T., *Meteorites: Their Record of Early Solar System History*, W. H. Freeman, New York, 1985.

Weidenschilling, S. J., Aerodynamics of solid bodies in the solar nebula, *Mon. Not. R. Astron. Soc., 180*, 57-70, 1977.

Weisberg, M. K., M. Prinz, R. N. Clayton, T. K. Mayeda, M. M. Grady, I. Franchi, C. T. Pillinger, and G. W. Kallemeyn, The K (Kakangari) chondrite grouplet, *Geochim. Cosmochim. Acta, 60*, 4253-4263, 1996.

Wen, C. Y., and Y. H. Yu, A generalized method for predicting the minimum fluidization velocity, *Am. Inst. Chem. Eng. J., 12*, 610-612, 1966a.

Wen, C.Y., and Y. H. Yu, Mechanics of fluidization, *Am. Inst. Chem. Eng. Symp. Ser., 62*, 100-111, 1966b.

Whipple, F. L., Accumulation of chondrules on asteroids, Physical Studies of Minor Planets, *NASA Spec. Publ., SP-267*, 251-256, 1971.

Whipple, F. L., On certain aerodynamic processes for asteroids and comets, in *From Plasma to Planet, Nobel Symp. 21*, edited by A. Elvius, pp. 211-232, John Wiley, New York, 1972.

Williams, J. C., The segregation of particulate materials. A review, *Powder Technol., 15*, 245-251, 1976.

Wilson, C. J. N., The role of fluidization in the emplacement of pyroclastic flows: An experimental approach, *J. Volcanol. Geotherm. Res., 8*, 231-249, 1980.

Wilson, C. J. N., The role of fluidization in the emplacement of pyroclastic flows, 2: Experimental results and their interpretation, *J. Volcanol. Geotherm. Res., 20*, 55-84, 1984.

Wilson, L. and K. Keil, Consequences of explosive eruptions on small solar system bodies: The case of the missing basalts on the aubrite parent body, *Earth Planet. Sci. Lett., 104*, 505-512, 1991.

Wood, J. A., Meteoritic constraints on processes in the solar nebula, in *Protostars and Planets II*, edited by D.C. Black, pp. 687-702, Univ. of Ariz. Press, Tucson, 1985.

Zhang, Y., S. Huang, D. Schneider, P. H. Benoit, J. M. DeHart, G. E. Lofgren, and D. W. G. Sears, Pyroxene structures, cathodoluminescence and the thermal history of the enstatite chondrites, *Meteorit. Planet. Sci., 31*, 87-96, 1996.

Zolensky, M., and H. Y. McSween Jr., Aqueous alteration, in *Meteorites and the Early Solar System*, edited by J. F. Kerridge and M. S. Matthews, pp. 114-143, Univ. of Ariz. Press, Tucson, 1988.

D. G. Akridge and D. W. G. Sears, Cosmochemistry Group, Department of Chemistry and Biochemistry, University of Arkansas, Fayetteville, AR 72701. (cosmo@cavern.uark.edu)

(Received March 2, 1998; revised February 24, 1999;
accepted March 3, 1999.)